Received: 23 June 2023 | Revised: 17 August 2023 | Accepted: 25 September 2023

DOI: 10.1002/alz.13514

Alzheimer's & Dementia®
THE JOURNAL OF THE ALZHEIMER'S ASSOCIATION

RESEARCH ARTICLE

Whole genome methylation sequencing in blood identifies extensive differential DNA methylation in late-onset dementia due to Alzheimer's disease

Coleman Breen[1] | **Ligia A. Papale**[2] | **Lindsay R. Clark**[3,4] | **Phillip E. Bergmann**[2] | **Andy Madrid**[2] | **Sanjay Asthana**[4,5] | **Sterling C. Johnson**[3,4,5] | **Sündüz Keleş**[1,6] | **Reid S. Alisch**[2] | **Kirk J. Hogan**[5,7]

[1]Department of Statistics, University of Wisconsin, Medical Sciences Center, Madison, Wisconsin, USA

[2]Department of Neurological Surgery, University of Wisconsin School of Medicine and Public Health, Madison, Wisconsin, USA

[3]Wisconsin Alzheimer's Disease Research Center, University of Wisconsin School of Medicine and Public Health, Madison, Wisconsin, USA

[4]Geriatric Research Education and Clinical Center, William S. Middleton Memorial Veterans Hospital, Madison, Wisconsin, USA

[5]Wisconsin Alzheimer's Institute, University of Wisconsin School of Medicine and Public Health, Madison, Wisconsin, USA

[6]Department of Biostatistics and Medical Informatics, University of Wisconsin School of Medicine and Public Health, Madison, Wisconsin, USA

[7]Department of Anesthesiology, University of Wisconsin School of Medicine and Public Health, Madison, Wisconsin, USA

Correspondence
Reid S. Alisch, Department of Neurological Surgery, University of Wisconsin–Madison School of Medicine and Public Health, 600 Highland Ave, Madison, WI 53792, USA.
Email: alisch@wisc.edu

Kirk J. Hogan, Department of Anesthesiology, University of Wisconsin–Madison School of Medicine and Public Health, B6/319 Clinical Science Center, 600 Highland Ave., Madison, WI 53792-3272, USA.
Email: khogan@wisc.edu

Funding information
National Institutes of Health, Grant/Award Numbers: R01AG066179, R01AG021155, R01AG027161, P30AG062715, HG003747, S10OD025245; Alzheimer's Association, Grant/Award Number: AARF19-614533; UW Department of Neurological Surgery; NLM, Grant/Award Number: 5T15LM007359

Abstract

INTRODUCTION: DNA microarray-based studies report differentially methylated positions (DMPs) in blood between late-onset dementia due to Alzheimer's disease (AD) and cognitively unimpaired individuals, but interrogate < 4% of the genome.

METHODS: We used whole genome methylation sequencing (WGMS) to quantify DNA methylation levels at 25,409,826 CpG loci in 281 blood samples from 108 AD and 173 cognitively unimpaired individuals.

RESULTS: WGMS identified 28,038 DMPs throughout the human methylome, including 2707 differentially methylated genes (e.g., *SORCS3*, *GABA*, and *PICALM*) encoding proteins in biological pathways relevant to AD such as synaptic membrane, cation channel complex, and glutamatergic synapse. One hundred seventy-three differentially methylated blood-specific enhancers interact with the promoters of 95 genes that are differentially expressed in blood from persons with and without AD.

DISCUSSION: WGMS identifies differentially methylated CpGs in known and newly detected genes and enhancers in blood from persons with and without AD.

Reid S. Alisch and Kirk J. Hogan contributed equally to this work.

KEYWORDS
Alzheimer's disease, blood DNA methylation, dementia, differentially methylated positions, whole genome methylation sequencing

Highlights

- Whole genome DNA methylation levels were quantified in blood from persons with and without Alzheimer's disease (AD).
- Twenty-eight thousand thirty-eight differentially methylated positions (DMPs) were identified.
- Two thousand seven hundred seven genes comprise DMPs.
- Forty-eight of 75 independent genetic risk loci for AD have DMPs.
- One thousand five hundred sixty-eight blood-specific enhancers comprise DMPs, 173 of which interact with the promoters of 95 genes that are differentially expressed in blood from persons with and without AD.

1 | BACKGROUND

Late-onset dementia due to Alzheimer's disease (AD) is diagnosed by signs and symptoms of dementia that occur at or after the age of 65. While the etiology of AD remains uncertain, recent evidence indicates that environmental influences increase the risk of AD in part through interactions with the epigenome.[1,2] Covalent addition of a methyl group at position 5 of the nucleotide cytosine generates 5-methylcytosine (5mC). 5mC participates in coordination of gene expression in the human genome. Fluctuations in 5mC levels across the genome are observed over the lifespan in association with cognitive aging and neurodegenerative diseases.[3] Variations in 5mC abundance and distribution have been identified in *post mortem* brain tissues of AD patients in genes that co-segregate with AD susceptibility.[4,5] Recent DNA microarray-based epigenome-wide association studies (EWAS) report differential methylation in known and newly recognized AD genes in brain and blood samples,[6–9] thereby underscoring the value of EWAS in disclosing novel genes and pathways associated with the pathogenesis of AD. Prior single gene-targeted and microarray-based studies used diverse DNA methylation detection platforms that query preselected genes and genomic regions, and scan at most only 3.4% of the potential methylated sites in the human genome.[10,11] A shared limitation of previous contributions is the use of DNA microarray-based technologies that are limited by a priori, biased choice of targeted loci, rather than use of unbiased, comprehensive methods of DNA methylation analysis using whole genome methylation sequencing (WGMS). As a preferred alternative to microarray-based methods, WGMS provides single base-pair resolution of all methylated sites in the linear DNA sequence of bases along the 5′ to 3′ direction in which a cytosine nucleotide is followed by a guanine nucleotide (CpG) in the human genome. This balanced approach supports evaluation of blood DNA methylation levels as potential molecular biomarkers of AD, and facilitates DNA methylation and multi-omic investigations with a pragmatic, translational opportunity to improve the diagnosis and individualized treatment of AD.

2 | METHODS

2.1 | Study participants

The experimental protocol was approved by the institutional review board (IRB) of the University of Wisconsin School of Medicine and Public Health, Madison, WI. All participants signed an IRB-approved informed consent.

2.1.1 | Wisconsin Alzheimer's Disease Research Center participants

The Wisconsin Alzheimer's Disease Research Center (WADRC) investigates AD in middle-aged to older adults from cognitively unimpaired to mild cognitive impairment (MCI) and AD. All participants are community dwelling and undergo serial examinations at the University of Wisconsin-Madison Hospital and Clinics.[12] WADRC Clinical Core participants undergo blood sample collection and comprehensive cognitive testing at annual or biennial intervals using the neuropsychological battery of the Uniform Data Set (UDS) comprising measures of attention, processing speed, executive function, episodic memory, language, and constructional ability.[13] A multi-disciplinary consensus conference panel reviews cognitive test findings and supporting information gathered at each study visit including medical history, depressive symptoms, self-reported memory functioning, social history, and informant reports of cognitive and functional status. Participants are classified as cognitively unimpaired, or meeting criteria for MCI or AD based on National Institute on Aging-Alzheimer's Association (NIA-AA) criteria.[14–16]

2.1.2 | Wisconsin Registry for Alzheimer's Prevention participants

Established in 2001, the Wisconsin Registry for Alzheimer's Prevention (WRAP) is an ongoing longitudinal observational cohort of initially dementia-free middle-aged participants who enroll at mid-life (mean age 54 at baseline) that is enriched with risk for late-onset AD due to parental history of AD dementia. Details of the study design and methods used have been previously described.[17] Participants are followed at serial intervals with detailed in-person assessments, questionnaires, and blood collection occurring at each study visit. The first follow-up is 4 years after a baseline visit with visits thereafter every 2 years. Participants remain in the study until they withdraw or develop another illness that precludes participation or accurate assessment of cognition. Each visit requires 5 hours and comprises cognitive measurements, anthropometric measures, laboratory tests, and questionnaire ratings completed by the participant and an informant including the Quick Dementia Rating System (QDRS) or Clinical Dementia Rating (CDR). Reliability and consistency of cognitive testing is established through regular review of aspects of testing procedures at team meetings, biannual individual observations of test administration, adherence to a standardized manual of procedures, and blinded rescoring by a separate rater (20% annually for each psychometrist). If cognitive abnormalities are detected by algorithm on neuropsychological tests, data from participant visits are brought to a consensus review committee consisting of dementia-specialist physicians, neuropsychologists, and nurse practitioners for in-depth review. Thresholds for committee review include performance greater than 1.5 standard deviation below robust internal norms adjusting for age, sex, and literacy level;[18–20] self-report or informant report of cognitive or functional decline on the CDR, the QDRS, the Informant Questionnaire on Cognitive Decline in the Elderly, or Instrumental Activities of Daily Living; or threshold-specific absolute scores on key tests (e.g., Wechsler Memory Scale–Revised Logical Memory-II 17, Rey Auditory Verbal Learning Test Delayed Recall ≤ 5, or Mini-Mental State Examination ≤ 26). The consensus committee assesses cognitive performance at all prior visits to detect intra-individual changes over time and analyzes pertinent findings from neurologic and physical examinations; laboratory values; medical and social histories; and self-survey of mood, cognition, and functional status. Participants are classified as cognitively unimpaired, or meeting criteria for MCI or AD based on NIA-AA criteria.[14–16]

2.1.3 | Selection of participants

All participants from the WADRC and WRAP with a consensus conference diagnosis of AD with available blood samples were included (Figure 1). Participants whose clinical diagnosis changed at a subsequent visit (e.g., reverted to cognitively unimpaired or was diagnosed as a non-AD dementia) were excluded. Cognitively unimpaired participants did not meet criteria for MCI or AD. Because of the younger age and larger proportion of women in the cognitively unimpaired sample, cognitively unimpaired women under age 65 were not included to closely match the MCI and AD cohorts for age and sex distribution.

RESEARCH IN CONTEXT

1. **Systematic review**: Recent DNA array studies with partial coverage reveal the association of methylome changes in blood in persons with Alzheimer's disease (AD), but there is a lack of systematic study of the entire human methylome.
2. **Interpretation**: We profiled whole genome-wide methylome variations in 281 blood samples from 108 AD and 173 cognitively unimpaired participants. We identified 28,038 differentially methylated positions (DMPs) in persons with AD compared to persons without AD. Forty-eight of 75 independent genetic risk loci for AD have one or more DMPs. Genomic enhancer sites are enriched for DMPs in persons with AD.
3. **Future directions**: In addition to investigation of samples from 101 persons with mild cognitive impairment, DMPs will be sought in archived longitudinal samples from the same persons collected every 2 years over 20 years, and in samples from persons with diverse ancestries.

2.2 | DNA extraction and generation of whole genome methylome data

Blood samples were acquired nearest to the date of AD diagnosis and matched for age by sample visit number in the cognitively unimpaired group. A 10 mL whole blood sample was anticoagulated in ethylenediaminetetraacetic acid and stored at −20°C. Genomic DNA was extracted using the Gentra Puregene Blood Core Kit C following the manufacturer's protocol (Catalog# 158389, Qiagen, Hilden, Germany). Seven hundred nanograms of sample of high molecular weight genomic DNA were forwarded to the University of Illinois at Urbana-Champaign Roy J. Carver Biotechnology Center for DNA sequence library construction using the NEBNext Enzymatic Methyl-seq (EM-seq) kit,[21] and whole genome sequencing on a next-generation sequencer (Illumina NovaSeq6000). Image processing and sequence extraction used the Illumina Pipeline. Raw fastq sequence files were forwarded to Dr. Alisch's laboratory via a secure website.

2.3 | Data processing

Data processing was performed with the ENCODE gemBS-based processing pipeline.[22] Raw WGMS data were analyzed with FastQC to ensure that all samples met quality control thresholds for sequencing

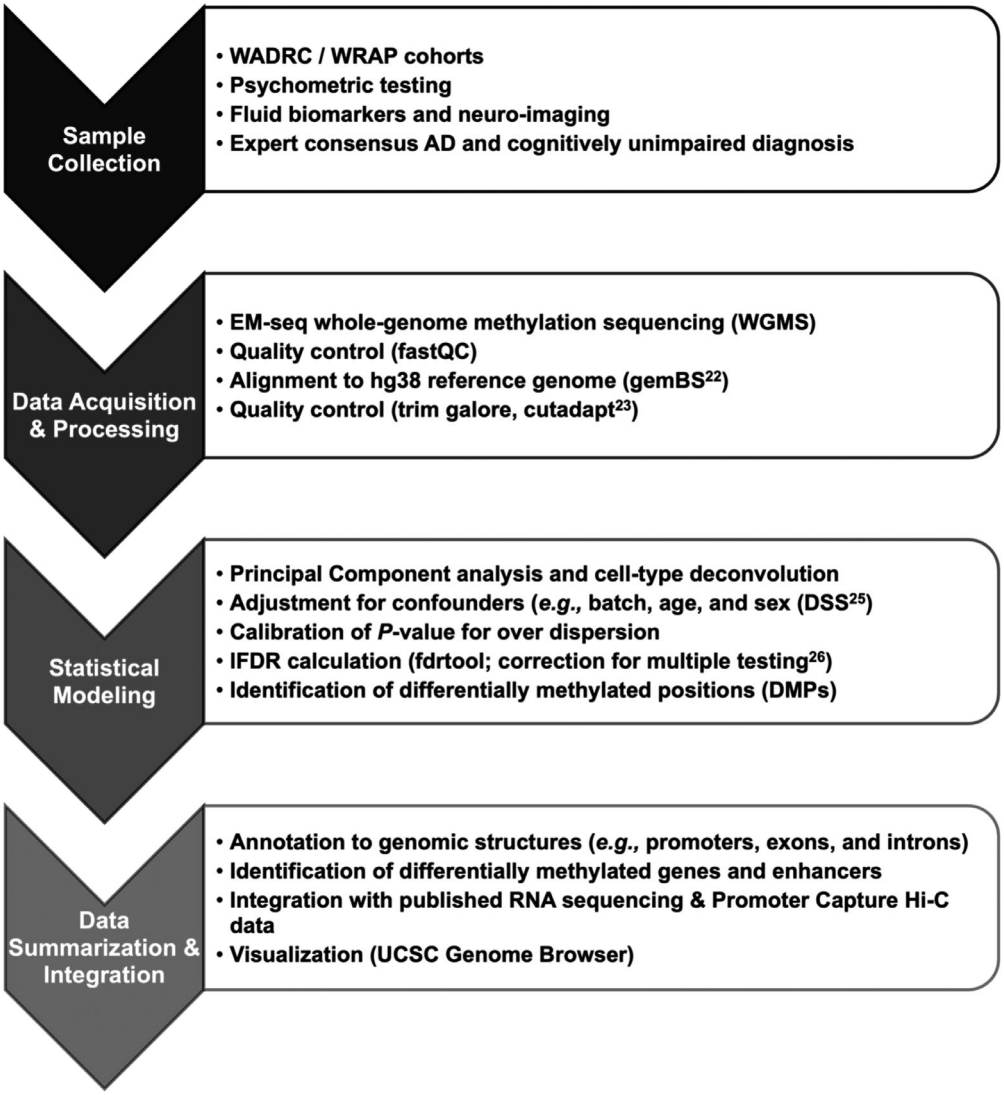

FIGURE 1 Flowchart depicting whole genome methylation sequencing (WGMS) data acquisition and analysis. AD, late-onset dementia due to Alzheimer's disease; LFDR, local false discovery rate; UCSC, University of California Santa Cruz; WADRC, Wisconsin Alzheimer's Disease Research Center; WRAP, Wisconsin Registry for Alzheimer's Prevention.

reads, and with Trim Galore to remove adapter content and to trim sequence reads.[23] DNA sequencing reads were aligned to GRCh38.14 (hg38) with gemBS[22] in pair-ended mode with default settings. Alignment with a "methylation-aware" sequence aligner provides counts for the number of reads supporting methylation and absence of methylation for each CpG locus. Methylated and unmethylated sequence read counts were merged across the two DNA strands of each sample. CpG loci were filtered to have median coverage of five or greater with 50% or less missing values among all participants. CpGs on sex chromosomes were removed from analysis. A total of 25,409,826 of 27,853,174 CpGs were retained after filtering and used in subsequent analyses. Missing values were imputed using diagnostic group averages (i.e., AD vs. cognitively unimpaired) at a specific CpG locus after merging across strands (Figure S1 in supporting information).

2.4 | Statistical analysis

2.4.1 | Cell-type deconvolution

Blood samples comprise a composite of different white blood cell types, each with a distinct methylomic signature. To adjust for leukocyte heterogeneity, we used reference-free deconvolution of subpopulations existing in methylation data (DXM)[24] to estimate the constituent fraction of each of the white blood cell types. To ensure the accuracy of these estimates, we then compared DXM cell type proportion estimates from the WGMS data to cell type proportion estimates in our published Illumina Infinium MethylationEPIC BeadChip Microarray (EPIC microarray) data[6] providing a shared subset of 83 participants with both WGMS and EPIC microarray data.

2.4.2 | Differential methylation analysis

Principal components (PC) were computed on the 5% of CpGs with greatest DNA methylation variability of each chromosome to assess potential batch effects between the WADRC and WRAP cohorts, age, and sex. Dispersion shrinkage for sequencing (DSS)[25] was used to fit a beta-binomial model for each CpG locus adjusted for estimated white blood cell proportions, the first two PCs, age, sex, and body mass index. An AD effect on methylation for each CpG was assessed with a Wald test of the corresponding regression coefficient. The empirical distribution of the 25,409,826 *P*-values resulting from the theoretical null (standard normal distribution) for the Wald test statistics of the CpGs deviated from the expected uniform distribution with an enrichment around small *P*-values. Accordingly, under-dispersed theoretical null test statistics ($\lambda_{GC} = 0.8$; Figure S2 in supporting information) were used to model the empirical null and calculate local false discovery rates (LFDRs) with fdrtool.[26] LFDRs were used to account for multiple testing and to aid interpretability. A CpG locus with a LFDR < 0.05 was identified as a differentially methylated position (DMP).

2.4.3 | Gene annotation, gene ontology analysis, and gene structure identification

5′ to 3′ genomic coordinates were obtained from ENSEMBL (v86).[27] Genes were defined as sequences spanning 3 kilobases (kb) 5′ of a transcription start site (TSS) to 200 base pairs (bp) 3′ of a transcription termination site (TTS). Gene promoters were identified within 5 kb 5′ of a TSS and 200 bp 3′ of a TSS. Two criteria were used to identify differential methylation in genes and promoters. First, each gene or promoter must comprise a gene-wide or promoter-wide LFDR < 0.01. To calculate gene-wide or promoter-wide LFDRs, *P*-values of each CpG within the gene or promoter are aggregated into a harmonic mean *P*-value.[28] The harmonic mean *P*-value controls the family-wise error rate of multiple statistical tests and does not assume independence among tests. The harmonic mean *P*-value thereby provides a preferred framework for aggregating *P*-values to correct for gene size (i.e., number of CpGs) and for highly correlated methylation levels of neighboring CpGs. This step is repeated for each gene and promoter yielding a single *P*-value for the entire gene or promoter. LFDRs are then calculated from the *P*-values to provide gene-wide and promoter-wide false discovery rates. The second criterion to test for differential methylation of genes and promoters requires at least one DMP defined as a CpG with an LFDR < 0.05 within the gene or promoter. Accordingly, genes and promoters with an LFDR < 0.01 and at least one DMP are identified as differentially methylated. Of note, this annotation may assign a DMP to more than a single gene with 936 of the 27,889 DMPs we observed annotated to two or more gene bodies. Gene Ontology (GO) analyses were performed with clusterProfiler (version 4.6.0),[29] which conducts an over-representation test.[28,30] False discovery rates are computed from *P*-values to account for multiple testing.

2.4.4 | Comparison to Illumina Infinium MethylationEpic BeadChip Microarray data

Of the 281 participants with WGMS data, 83 were included in a previous study that used the EPIC microarray to quantify methylation levels across > 850,000 CpGs spanning the human genome.[6] Methylation values from the EPIC microarray platform were lifted to hg38 and matched to WGMS data. A total of 799,629 loci were quantified with both technologies for all 83 shared samples. A Pearson correlation coefficient was calculated to test for concordance between the EPIC microarray and WGMS assays.

2.4.5 | Differential methylation analysis of blood promoter–enhancer interactions

To identify differential methylation in gene promoter and enhancer regions, promoter–enhancer interactions in white blood cells were examined using Promoter Capture Hi-C (PCHi-C) data.[31] An interaction was considered significant if the minimum CHiCAGO score across all blood cell types was > 5.[31] Interactions were filtered to have a median CHiCAGO score > 5 across all blood cell types to ensure adequate signal. After removal of false positive (e.g., bait–bait) and sex chromosome interactions, remaining promoter/enhancer interactions were lifted over to the human genome version GRCh38 with the UCSC liftOver tool.[32] This approach retained 104,554 promoter–enhancer interactions comprising 9631 distinct promoters and 58,654 distinct enhancers for comparison to WGMS data. Promoters and enhancers were considered differentially methylated if they contained one or more DMPs. Over- or under-representation of DMPs in enhancer regions were tested against a null distribution generated by random sampling of a set of 28,038 simulated DMPs from the 25,409,826 CpGs. The empirical null distribution quantified the proportion of DMPs located within a blood enhancer based on 10,000 random Monte Carlo samplings. A two-tailed test statistic was calculated to ascertain the number of DMPs occurring within an enhancer by chance alone. The same simulation procedure was also used to identify under- or over-representation of DMPs in promoters.

2.4.6 | Comparison of differential methylation and differential expression in AD

To evaluate whether genes defined as above with one or more DMPs in one or more promoter–enhancer interactions were differentially expressed between AD versus cognitively unimpaired persons, we compared WGMS data to published transcriptome data that identified 846 differentially expressed genes in blood associated with AD.[33] After removal of differentially expressed genes on sex chromosomes, 790 were retained for subsequent analyses. Differentially expressed genes were then correlated with differentially methylated genes,

TABLE 1 Means and (standard deviations) for cognitively unimpaired and AD demographic variables. *t* statistics and corresponding *P*-values are reported for two-group comparisons.

Phenotype	CU 173	AD 108	Statistical test
No *APOE* ε4	129	40	$\chi^2 = 45.61; p < 10^{-9}$
Heterozygous *APOE* ε4	39	47	
Homozygous *APOE* ε4	4	20	
Age (years)	69.8 (7.5)	73.3 (9.8)	$t = -3.11; p < 0.01$
Education (years)	16.7 (2.6)	15 (2.8)	$t = 5.1; p < 10^{-6}$
Body mass index (kg/m^2)	28.7 (5.2)	26.7 (4.8)	$t = 3.28; p < 0.01$
WADRC	127	103	$p < 10^{-5}$
WRAP	46	5	
American Indian or Alaska Native	1	0	$p = 0.74$
Black or African American	7	6	
White	165	102	
Female	90	47	$\chi^2 = 1.60; p = 0.21$
Male	83	61	

Note: A chi-squared test statistic was used to test independence for *APOE* heterozygote and homozygote status. Two study participants were not genotyped and are not included in statistical test for *APOE* status. Fisher exact test was used to test independence for self-identified ancestry with zero counts in some groups.
Abbreviations: AD, late-onset dementia due to Alzheimer's disease; *APOE*, apolipoprotein E; CU, cognitively unimpaired; WADRC, Wisconsin Alzheimer's Disease Research Center; WRAP, Wisconsin Registry for Alzheimer's Prevention.

differentially methylated enhancer genes, and differentially methylated promoter genes by gene symbol.

2.4.7 | Software for statistical analysis and data visualization

All statistical analyses were conducted in R (4.2.2). Figures were generated with ggplot2 (3.4.0),[34] ggsci (2.9),[35] and cowplot (1.1.1).[36]

3 | RESULTS

3.1 | Study participants

A total of 281 WADRC and WRAP participants comprising 108 AD and 173 cognitively unimpaired participants were included in the present analysis. Forty-four percent of participants with AD were female compared to 52% female participants without AD (Table 1). Participants with AD were about 3 years older than the participants without AD, with approximately 2 fewer years of education and two lower body mass points. All but 14 participants reported European ancestry. Twenty-two participants with AD were apolipoprotein E (*APOE*) ε4 homozygotes compared to four cognitively unimpaired individuals. Forty-seven participants with AD were *APOE* ε4 heterozygotes compared to 39 cognitively unimpaired.

3.2 | Whole genome DNA methylation detection in persons with and without AD

After filtering for quality assurance, EM-seq generated an average of 558 million paired-end sequence reads for each sample. An average of 554 million sequence reads uniquely mapped to the human genome (GRCh38.14 [hg38]) providing an average genomic coverage of 56.6x, with a mean of 38.7x and a median 38.4x effective coverage after merging across strands for interrogation of 25,409,826 CpGs (Figure S1). We previously reported the DNA methylation levels of a subset of the present participants ($N = 83$) using the EPIC microarray.[6] DNA methylation levels at 799,629 CpGs shared between the WGMS data and microarray data were highly correlated (Pearson correlation coefficient = 0.97; *P*-value < 0.001), indicating that the two platforms detect nearly identical DNA methylation levels spanning the genome.

To identify DMPs between persons with and without AD, each CpG locus was modeled with a generalized linear model using the DSS software, an implementation of the beta-binomial model designed for DNA methylation analysis.[25] Cell-type proportions for each sample estimated with DXM were highly correlated with microarray-based data (Figure S3 in supporting information).[37] Batch effects in WGMS data tested using the first two PCs accounted for 4% and 2% of total variability, respectively. No batch effects for cohort (WADRC or WRAP), diagnosis (AD or cognitively unimpaired), sex, or self-identified ancestry covariates were observed (Figure S4 in supporting information).

3.3 | Extensive differential DNA methylation across the AD genome

DNA methylation levels in blood that differ between persons with and without AD are observed at > 0.1% (28,038) of all CpG loci that comprise the human methylome (27,853,174; Figure 2). DMPs are distributed in all genomic regions with 60.5% residing within a gene intron. Fewer than 3% of DMPs are located within 1 kb 5′ of the TSS. More than 90% of DMPs are located > 4 kilobases away from a CpG island. A total of 1333 DMPs have an absolute mean difference in DNA methylation greater than 5% between persons with and without AD (Table S1 in supporting information). Eighty-four percent of AD DMPs are hypomethylated. Sixty-four percent (48/75) of AD genomic risk loci recently reported in a large genome-wide association study (GWAS)[38] comprise DMPs (Table S2 in supporting information).

3.4 | Differential DNA methylation in recognized AD genes

To test whether DNA methylation levels in blood differ in genes highly correlated with the onset and progression of early-onset AD, we

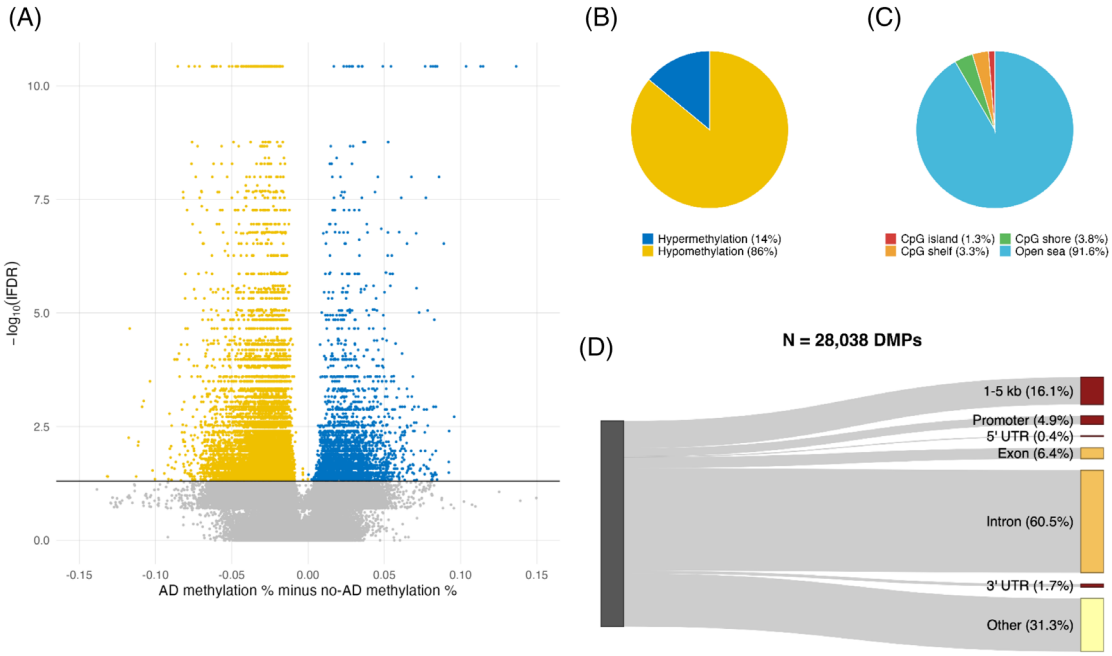

FIGURE 2 Identification of 5′-cytosoine-phosphate-guanine-3′ (CpG) loci that comprise differentially methylated positions (DMPs) in blood from participants with and without Alzheimer's disease (AD). (A) Volcano plot of 25,409,826 WGMS CpG loci depicting the difference in mean methylation percent (x-axis) and the significance (y-axis, local false discovery rate [LFDR]). Each point corresponds to a single CpG locus. Yellow points indicate hypomethylated DMPs. Blue points indicate hypermethylated DMPs. Gray points indicate CpG loci that are not differentially methylated between persons with and without AD. The string of yellow and blue points across the top of the plot have reached the minimum LFDR as computed by fdrtool.[26] (B) Pie chart depicting the percentage of hypomethylated (86%) and hypermethylated (14%) AD-associated DMPs. (C) Pie chart depicting the locations of DMPs relative to CpG islands, CpG island shores 0–2 kb from CpG island edges, CpG island shelves 2–4 kb from CpG island edges, and open seas 4 kb or more from an CpG island edge. (D) Sankey plot depicting the locations of 28,038 AD-associated DMPs relative to genomic structures comprising 1-5 kilobases (kb) upstream of the transcription start site (TSS; "1-5 kb"), up to 1 kb upstream of the TSS ("promoter"), the 5′ untranslated region ("5′ UTR"), the 3′ untranslated region ("3′ UTR"), and 5 kb or more from any gene structure ("Other").

quantified differential DNA methylation in a panel of AD loci. To bracket 5′ and 3′ untranslated regions (UTRs) and promoter sequences, we examined each gene 3 kilobases 5′ from its TSS and 200 base pairs 3′ from its TTS. AD-associated genes including translocase of outer mitochondrial membrane 40 (*TOMM40*),[39] presenilin 1 (*PSEN1*),[40] amyloid beta precursor protein (*APP*),[40] and microtubule associate protein tau (*MAPT*)[41] comprise 1, 1, 2, and 4 DMPs, respectively (Figure 3). No DMPs were observed in presenilin 2 (*PSEN2*)[40] or *APOE*[42] genes.

3.5 | Differentially methylated genes in blood between persons with and without AD

Genomic annotation of differential methylation between persons with and without AD identifies 2707 differentially methylated genes, that is, 14% of human genes,[43] with many genes having multiple DMPs including signal-regulatory protein beta-1 (*SIRPB1*; 18 DMPs), NIPA magnesium transporter 2 (*NIPA2*; 22 DMPs), and thymine DNA glycosylase (*TDG*; 18 DMPs; P-value < 0.01, Figure 4, Table S3 in supporting information). Whereas a single DMP is present in many recognized AD-associated genes (e.g., sortilin related VPS10 domain containing receptor 3 [*SORCS3*]),[44] other genes comprise one or more clusters of DMPs (e.g., *TDG*) and dopamine receptor-regulating factor/Kruppel-like factor 16 (*KLF16*).[45] Differential DNA methylation also occurs as clusters of DMPs in contiguous gene groups (Figure 4), that is, heterogeneous nuclear ribonucleotide protein C (*HNRNPC*), retinitis pigmentosa GTPase regulator interacting protein (*RPGRIP1*), SPT16 homolog, facilitates chromatin remodeling subunit (*SUPT16H*), chromodomain helicase DNA binding protein 8 (*CHD8*), Ras-associated protein 2B (*RAB2B*), and tox high mobility group box family member 4 (*TOX4*).

To examine the potential biological significance of the 28,038 AD-associated differentially methylated genes, we performed a pathway enrichment analysis. Multiple terms with biological relevance to AD were identified including synaptic membrane, cation channel complex, glutamatergic synapse, and postsynaptic membrane (Figure 5; Table S4 in supporting information). Multiple differentially methylated genes discovered in these pathways have previously recognized links to AD, including *PICALM*, *GABA*, and *SORCS3*.[44,46,47]

3.6 | AD-related DMPs reside within interactions between blood-specific enhancers and promoters

To test the hypothesis that DMPs located > 5 kb outside of a gene boundary and its putative promoter (i.e., 31.3% of DMPs) may

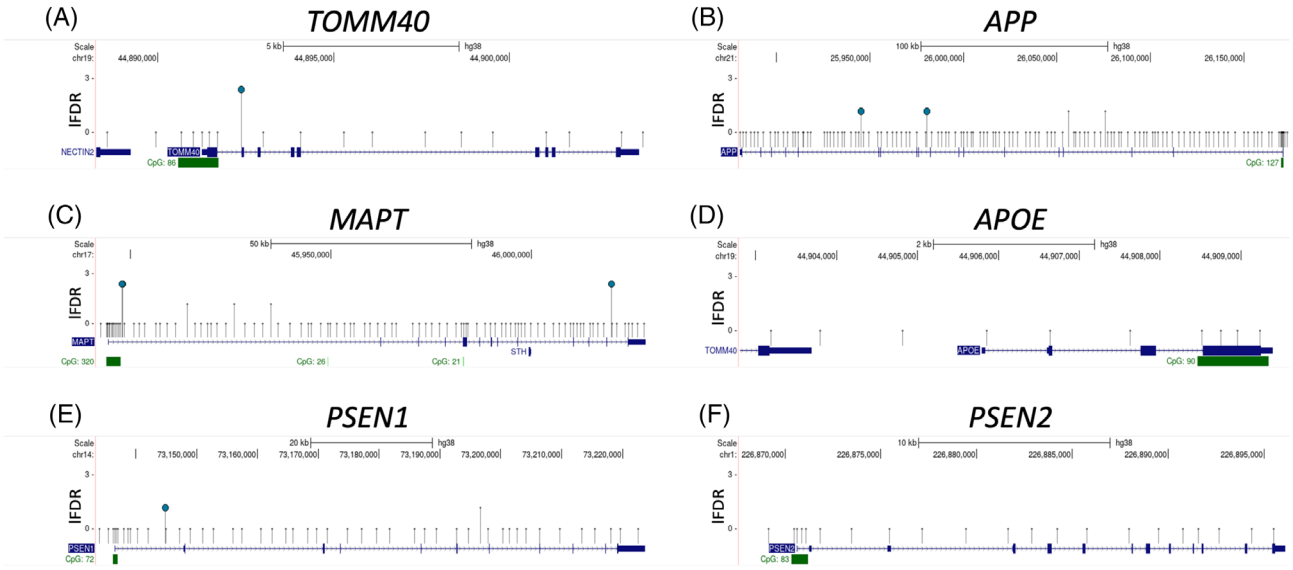

FIGURE 3 Differentially methylated positions (DMPs) in Alzheimer's disease (AD)-related genes. University of California Santa Cruz (UCSC) Genome Browser views of the methylome landscapes of representative AD-associated genes. (A–F) Sense strands are depicted with gene name abbreviations above each panel. (Please see Section 3.4 for gene nomenclature.) The 5′ to 3′ genome window for the schematic diagrams spans 3 kilobases (kb) 5′ of the transcription start site (TSS) to 200 base pairs (bp) 3′ of the transcription termination site (TTS). Alignment to human reference genome (hg38) coordinates are in bp. The scales of x-axis linear sequences in kb of each gene region are indicated at the top of each panel. Significance is indicated by local false discovery rate (LFDR) on the y-axis, with longer stems and large light blue circles to indicate hypermethylation. A corrected significance level of LFDR < 0.05 was adopted for all comparisons. One in 25 non-significant 5′-cytosoine-phosphate-guanine-3′ (CpGs) in each region are depicted as small stems and small gray circles. Dark blue rectangles indicate coding (taller rectangle) and non-coding (shorter rectangle) exons. The direction of gene transcription and introns are depicted by small dark blue arrows on the x-axis. CpG islands > 300 bp in length are indicated by dark green rectangles and CpG islands < 300 bp are indicated by light green rectangles beneath each panel. The number of CpGs in each island is shown to the left of each green rectangle. * indicates three overlapping DMPs in *MAPT*.

contribute to gene expression, we examined 58,654 published blood-specific enhancer–promoter interactions[48] for DMP enrichment in enhancers and promoters. We observed 1568 and 647 differentially methylated enhancers and promoters, respectively (*P*-value < 0.001, Tables S5 and S6 in supporting information), including a significant number (307) of promoter–enhancer interactions with DMPs in both the enhancer and promoter (chi-square test of independence *P*-value < 0.001). Comparison of these data with published differential RNA expression data in blood from persons with and without AD shows that 173 of the 1568 DMP-containing enhancers have long-range interactions with 95 promoters of genes known to be differentially expressed in blood of AD patients, including *B4GALT1* (Figure 6, Tables S5 and S6 in supporting information).[33,49] Differentially methylated enhancers interact with the promoters of 13 out of 75 AD genetic risk loci,[38] including 7 AD genes not otherwise found to be differentially methylated in our analysis (Section 3.3). Accordingly, either the gene bodies or the enhancers of 55 of 75 AD genetic risk loci are differentially methylated in blood.

4 | DISCUSSION

Multiple investigations report the association of differential DNA methylation in blood with the diagnosis of AD in independent cohorts.[9] Using single nucleotide resolution whole genome methylation sequencing, we conducted the first comprehensive investigation of differential DNA methylation levels in blood from participants with and without AD (Figure 1). We identified significant correlations of DNA methylation levels with the diagnosis of AD at 28,038 DMPs comprising 0.1% of 25,409,826 CpG candidates for differential methylation in the human genome after adjusting for technical and demographic variables (Table 1), and correction for multiple testing (Table S1). In keeping with global hypomethylation and regional hypermethylation of the human methylome with age, 86% of AD-associated DMPs were hypomethylated, suggesting advanced aging in AD patients (Figure 2A).[50] Finding that > 90% of AD-related DMPs are found further than 4 kb away from a CpG island underscores the importance of differential DNA methylation detection with WGMS rather than with microarray-based platforms that target CpG islands.

Genomic annotation of differential methylation in blood from persons with and without AD identifies 2707 differentially methylated genes, that is, 14% of genes in the human genome.[43] Gene products of specific genes that comprise newly discovered AD-associated DMPs are reported to participate in pathways with previously recognized links to AD, including *KLF16*, which regulates dopamine receptors.[45] Other genes have no prior established links to AD pathogenesis, such as *TDG*, *CHD8*, *RAB2B*, and *TOX4*. Of note, certain genes comprising DMPs that lack presently recognized links to AD pathogenesis

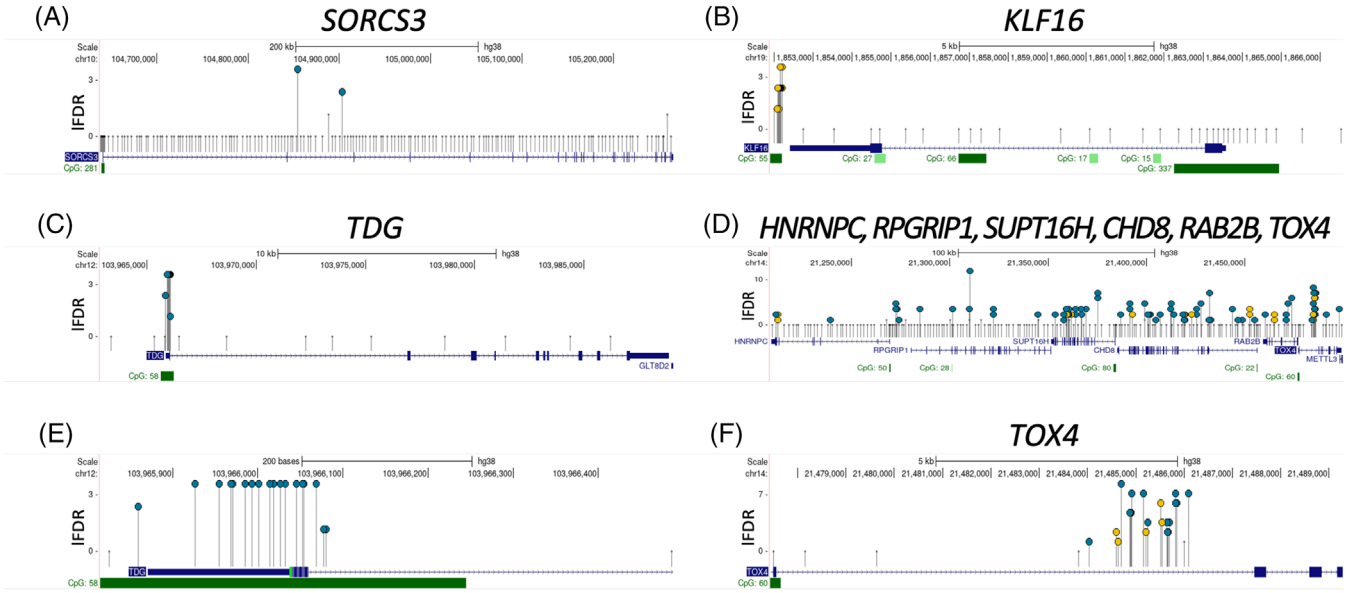

FIGURE 4 Genes with 5′-cytosoine-phosphate-guanine-3′ (CpGs) that are differentially methylated (DMPs) between persons with and without late-onset dementia due to Alzheimer's disease (AD). University of California Santa Cruz (UCSC) Genome Browser views of the methylome landscapes of representative AD-associated genes (A–F) are depicted with gene name abbreviations above each panel. (Please see Section 3.5 for gene nomenclature.) The 5′ to 3′ genome window for (A) *SORCS3* (sense strand) and (C) *TDG* (sense strand) spans three kilobases (kb) 5′of the transcription start site (TSS) to 200 base pairs (bp) 3′ of the transcription termination site (TTS). Note that the genomic window for (B) *KLF16* (anti-sense strand) spans 3 kb 5′ of the TSS to 500 bp 3′ of the TTS to comprise a DMP cluster. (D) shows a six-gene region comprising *HNRNPC*, *RPGRIP1*, *SUPT16H*, *CHD8*, *RAB2B*, and *TOX4* that spans 200 bp downstream of the *HNRNPC* TTS to 200 base pairs (bp) 3′ of the *TOX4* TTS. (E) depicts an expanded region of *TDG* comprising a plurality of DMPs in exon 1. (F) depicts an expanded region of *TOX4* comprising a plurality of DMPs. Alignment to human reference genome (hg38) coordinates are in in bp, and the scales of x-axis linear sequences in kb of each gene region are indicated at the top of each panel. Significant differences in local false discovery rates (LFDR) adjusted DNA methylation *P*-values are provided on the y-axis, with longer stems and large light blue circles to indicate hypermethylation, and large yellow circles to indicate hypomethylation. A corrected significance level of LFDR < 0.05 was adopted for all comparisons. One in 25 non-significant DMPs in each region are depicted as small stems and small gray circles. Dark blue rectangles indicate exons. The direction of gene transcription and introns are depicted by small dark blue arrows on the x-axis. CpG islands > 300 bp are indicated by dark green rectangles and CpG islands < 300 bp by light green rectangles beneath each panel. The number of CpGs in each island is shown to the left of each green rectangle.

directly participate in methylation (e.g., *CHD8*)[51] and de-methylation (e.g., *TDG*)[52] pathways. Together, these results suggest that differential DNA methylation levels in blood may be molecular biomarkers of AD susceptibility and expression.

Ontological pathway enrichment analysis of the 2707 AD-associated differentially methylated genes identified pathways with previously recognized links to AD, including *SORCS3*, which is differentially expressed in *post mortem* AD brain and is involved in APP processing with important roles in memory formation and synaptic plasticity,[44] *GABA* with impaired expression in AD brain tissue (e.g., hippocampus, subiculum, entorhinal cortex, and superior temporal gyrus[46]), and *PICALM*, a clathrin-adaptor protein that plays critical roles in clathrin-mediated endocytosis and in autophagy, and that modulates brain amyloid beta (Aβ) pathology and tau accumulation.[47]

Enhancers are *cis*- and *trans*-acting regions of the human genome that coordinate cell-type–specific gene expression by looping long distances to reach physical proximity with the promoters of their target genes.[48] Differential methylation in enhancers corresponds to disease status in a diversity of clinical settings.[53–55] Finding 1568 differentially methylated blood-specific enhancers[31] comprising 173 that interact with the promoters of 95 genes linked to differential RNA expression[33] in blood samples from participants with AD suggests that differential DNA methylation levels influence long-range gene expression related to AD pathogenesis. Further investigation is required to resolve the mechanistic interplay between cell-type–specific DNA methylation, long-range enhancer-mediated gene expression, and AD. For example, single-cell transcriptomics including scMT-seq[56] simultaneously measure gene expression and differential DNA methylation of gene bodies, enhancers, and promoters. As well, differential DNA methylation of gene bodies, enhancers, and promoters in serial longitudinal samples as participants progress along cognitive trajectories will serve to identify which interactions are of greatest functional importance. In particular, cross-tissue and cross cell–type comparisons using WGMS in blood and *post mortem* brain samples from the same participants will further identify long-range interactions with diagnostic and prognostic utility.[57]

Our data indicate that many more loci of the human methylome are responsive to and may participate in AD expression than indicated by earlier reports using circumscribed microarray-based DNA platforms that query < 4% of CpGs that are eligible for differential methylation.[9] While DNA methylation levels alone cannot suffice to conclusively test for mechanisms of AD pathophysiology, our data provide an essential

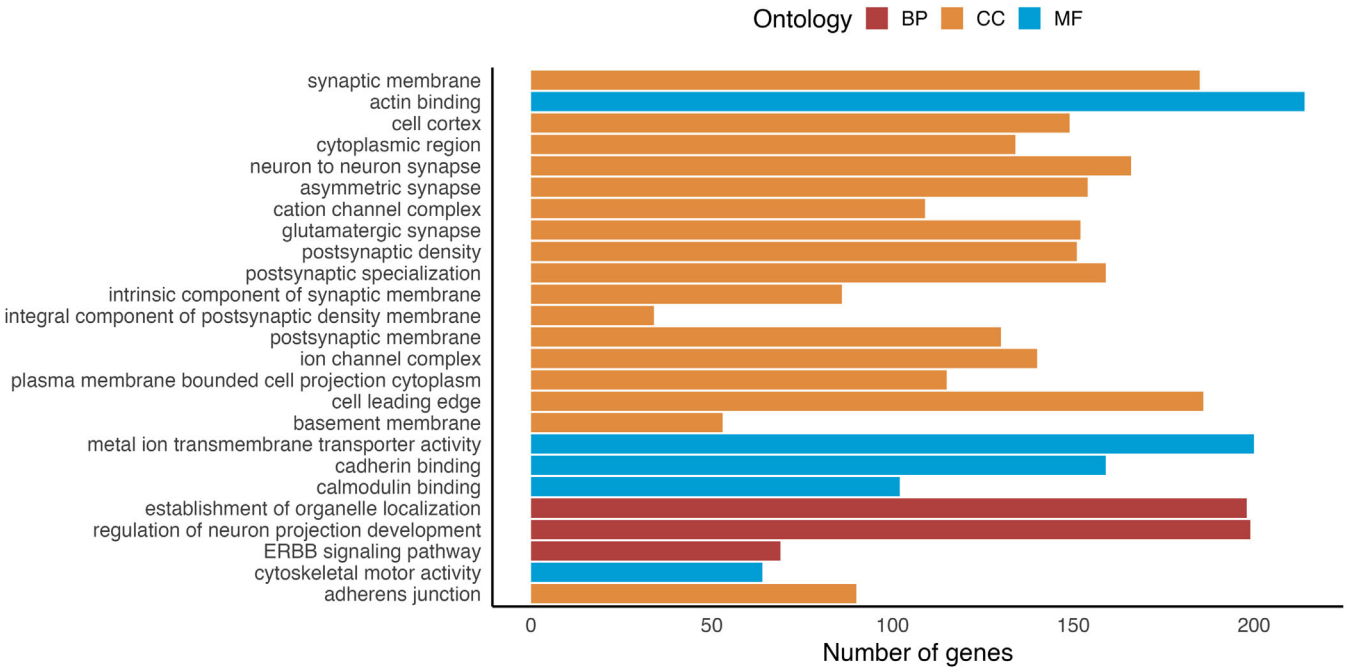

FIGURE 5 Ontological pathway analysis of genes comprising differential DNA methylation levels (DMPs) between persons with and without late-onset dementia due to Alzheimer's disease (AD). The top 25 terms (y-axis) by significance (local false discovery rate [LFDR] < 0.05) are depicted and arranged by gene set size found following annotation of DMP-associated genes (x-axis) to ontological pathways. BP, biological process; CC, cellular component; MF, molecular function.

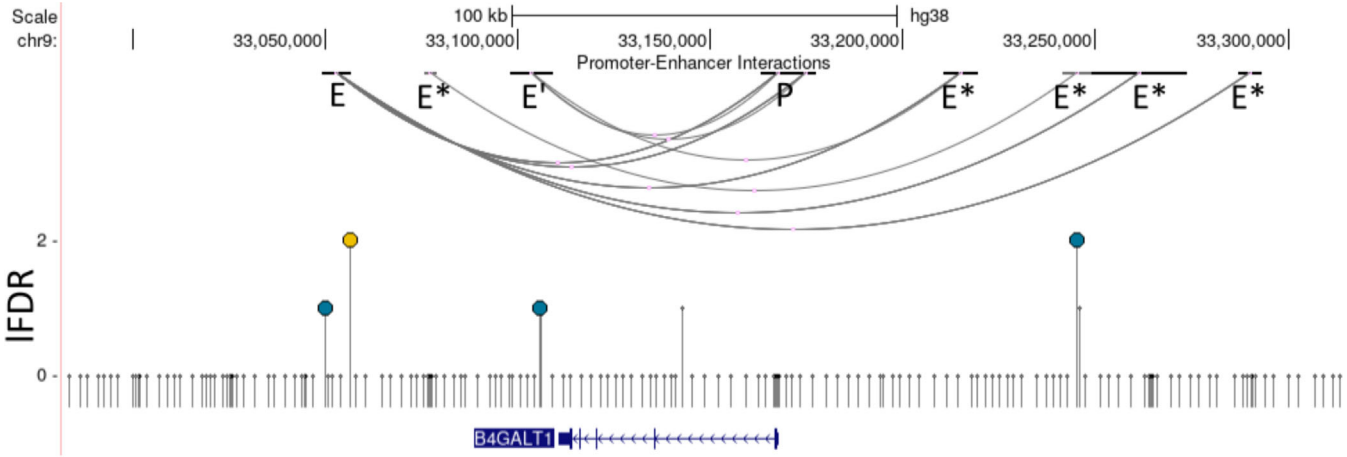

FIGURE 6 Long-range interactions with *B4GALT1* (anti-sense strand), a gene that is differentially expressed in the blood of persons with late-onset dementia due to Alzheimer's disease.[33] The relative scale (in kilobases [kb]) and genomic coordinates (in base pairs [bp]) of the region are provided at the top of panel, and the relative location of *B4GALT1* is shown at the bottom of panel. The black line with arrowheads shows the transcription direction. Significant differences in local false discovery rate (LFDR) adjusted DNA methylation *P*-values are provided on the y-axis, with longer stems and large light blue circles to indicate hypermethylation, and large yellow circles to indicate hypomethylation. A corrected significance level of $P < 0.05$ was adopted for all comparisons. One in 25 non-significant DMPs in each region is depicted as small stems and small gray circles. Enhancers (E and E') interact with the *B4GALT1* promoter (P), while specific enhancers (E*) interact with other enhancers. chr = chromosome.

substrate for future combined methylomic, genomic, transcriptomic, proteomic, and metabolomic investigations with potential to disclose etiologic contributors and to discern personalized AD trajectories at high levels of resolution.[58] As well, panels of validated whole methylome DMP molecular biomarkers of AD in blood may be configured for translation to clinical and research applications using targeted, rapid, minimally invasive, and cost efficient DMP detection platforms.

Our study has multiple strengths. AD and cognitively unimpaired phenotypes in WRAP and WADRC are assigned based on shared, stringent, well-validated, and consensual clinical and psychometric criteria.

WGMS performed with enzyme conversion of unmethylated cytosines rather than harsher sodium bisulfite treatment[21] generated exceptional genomic coverage of 56.6x (Figure S1).[59] WGMS supports comprehensive resolution of whole methylome CpGs using sequencing-by-synthesis compared to partial coverage of hybridization-based microarray methods with loci and probes selected for commercial utility.[9] Rigorous statistical approaches confirmed consistent cell type proportion estimates and the absence of batch effects (Figures S3, S4). As well, we used LFDRs from aggregated *P*-values as preferred and conservative inferential analytics. Finally, our sample sizes are substantial, and our adjustments for known confounders and corrections for multiple comparisons are robust.

Our study also has limitations. Although circulating monocytes and macrophages have recently been shown to participate in blood–brain barrier disruption and AD cellular pathology,[60–62] associations between DNA methylation in blood leukocytes and brain neurons and glia must only be drawn with great care and strong experimental support. Despite highly significant correlation of DNA methylation levels between our published microarray data and the present WGMS data in 83 participants, only 13 of 106 differentially methylated genes observed using the EPIC microarray platform were also identified using WGMS.[6] While this finding may be accounted for by differences in experimental methods including sample sizes, detection technologies, and statistical models, it suggests that comparisons between DNA methylation microarray and sequence data warrant close scrutiny. Importantly, it is not possible to distinguish the causal role of DNA methylation alterations in blood samples from persons with AD. Although our data show that 14% of coding genes are differentially methylated in persons with AD perhaps in keeping with the profound years-long and body-wide devastation of the disease, it is not possible to resolve changes that are causal from those that are compensatory or consequential based on cross-sectional DNA methylation data standing alone. Parallel investigations of differential DNA methylation in persons with AD from diverse ethnicities is a high priority for future studies.

In summary, WGMS revealed 28,038 CpG loci that are differentially methylated between AD and cognitively unimpaired individuals using conservative diagnostic clinical and psychometric thresholds and protected inferential statistical methods. These data provide the first analysis of differences in DNA methylation in blood between participants with and without AD using single nucleotide resolution WGMS. If replicated by others, our WGMS data offer the potential to guide and coordinate AD gene expression research at a new level of resolution interposed between the static genome and the dynamic environment. In turn, panels of AD-associated DMPs hold promise to serve as individualized molecular biomarkers of AD susceptibility, onset, progression, and response to targeted interventions.

5 | CONCLUSIONS

Single nucleotide resolution whole genome methylation sequencing in blood identifies far-reaching differential DNA methylation in late-onset dementia due to AD and underscores the use of unbiased investigations of the human genome. These findings provide the foundation for integration of multi-omic data for the development of pragmatic, translational tools toward improved diagnosis and individualized treatment of AD.

ACKNOWLEDGMENTS

The authors would like to thank the participants and study personnel who made this work possible. This work was supported by the National Institutes of Health grant numbers: R01AG066179; R01AG021155; R01AG027161; P30AG062715; HG003747; and S10OD025245, and the Alzheimer's Association AARF19-614533 and the UW Department of Neurological Surgery. CB was supported by an NLM training grant 5T15LM007359. The funding sources had no role in the design, collection, analysis and interpretation of the data, writing the report, or decision to submit the article for publication.

CONFLICT OF INTEREST STATEMENT

Sterling Johnson has served on advisory boards for Roche Diagnostics and Eisai. Dr. Johnson has participated on an advisory panel for and received an equipment grant from Roche Diagnostics, and he has received support (sponsoring of an observational study and provision of precursor for tau imaging) from Cerveau Technologies. The remaining authors have no relevant disclosures. Author disclosures are available in the supporting information.

CONSENT STATEMENT

The experimental protocol was approved by the institutional review board (IRB) of the University of Wisconsin School of Medicine and Public Health, Madison, WI. All participants signed an IRB-approved informed consent.

REFERENCES

1. Bennett DA, Yu L, Yang J, Srivastava GP, Aubin C, De Jager PL. Epigenomics of Alzheimer's disease. *Transl Res*. 2015;165:200-220.
2. Gao X, Chen Q, Yao H, et al. Epigenetics in Alzheimer's Disease. *Front Aging Neurosci*. 2022;14:911635.
3. Sanchez-Mut JV, Heyn H, Vidal E, et al. Human DNA methylomes of neurodegenerative diseases show common epigenomic patterns. *Transl Psychiatry*. 2016;6:e718.
4. Younesian S, Yousefi AM, Momeny M, Ghaffari SH, Bashash D. The DNA methylation in neurological diseases. *Cells*. 2022;11.
5. Lang AL, Eulalio T, Fox E, et al. Methylation differences in Alzheimer's disease neuropathologic change in the aged human brain. *Acta Neuropathol Commun*. 2022;10:174.
6. Madrid A, Hogan KJ, Papale LA, et al. DNA hypomethylation in blood links B3GALT4 and ZADH2 to Alzheimer's disease. *J Alzheimers Dis*. 2018;66:927-934.
7. Wang E, Wang M, Guo L, et al. Genome-wide methylomic regulation of multiscale gene networks in Alzheimer's disease. *Alzheimers Dement*. 2023;19:3472-3495.
8. Kim BH, Vasanthakumar A, Li QS, et al. Integrative analysis of DNA methylation and gene expression identifies genes associated with biological aging in Alzheimer's disease. *Alzheimers Dement (Amst)*. 2022;14:e12354.
9. Peng X, Zhang W, Cui W, Ding B, Lyu Q, Wang J. ADmeth: a manually curated database for the differential methylation in Alzheimer's

disease. *IEEE/ACM Trans Comput Biol Bioinform*. 2023;20:843-851.
10. Fransquet PD, Lacaze P, Saffery R, et al. DNA methylation analysis of candidate genes associated with dementia in peripheral blood. *Epigenomics*. 2020;12:2109-2123.
11. CS T, Young JI, Zhang L, et al. Cross-tissue analysis of blood and brain epigenome-wide association studies in Alzheimer's disease. *Nat Commun*. 2022;13:4852.
12. Allison SL, Jonaitis EM, Koscik RL, et al. Neurodegeneration, Alzheimer's disease biomarkers, and longitudinal verbal learning and memory performance in late middle age. *Neurobiol Aging*. 2021;102:151-160.
13. Weintraub S, Besser L, Dodge HH, et al. Version 3 of the Alzheimer disease centers' neuropsychological test battery in the uniform data set (UDS). *Alzheimer Dis Assoc Disord*. 2018;32:10-17.
14. McKhann GM, Knopman DS, Chertkow H, et al. The diagnosis of dementia due to Alzheimer's disease: recommendations from the National Institute on Aging-Alzheimer's Association workgroups on diagnostic guidelines for Alzheimer's disease. *Alzheimers Dement*. 2011;7:263-269.
15. Albert MS, DeKosky ST, Dickson D, et al. The diagnosis of mild cognitive impairment due to Alzheimer's disease: recommendations from the National Institute on Aging-Alzheimer's Association workgroups on diagnostic guidelines for Alzheimer's disease. *Alzheimers Dement*. 2011;7:270-279.
16. Clark LR, Berman SE, Norton D, et al. Age-accelerated cognitive decline in asymptomatic adults with CSF beta-amyloid. *Neurology*. 2018;90:e1306-e1315.
17. Johnson SC, Koscik RL, Jonaitis EM, et al. The Wisconsin registry for Alzheimer's prevention: a review of findings and current directions. *Alzheimers Dement (Amst)*. 2018;10:130-142.
18. Clark LR, Koscik RL, Nicholas CR, et al. Mild cognitive impairment in late middle age in the Wisconsin registry for Alzheimer's prevention study: prevalence and characteristics using robust and standard neuropsychological normative data. *Arch Clin Neuropsychol*. 2016;31:675-688.
19. Berman SE, Koscik RL, Clark LR, et al. Use of the quick dementia rating system (QDRS) as an initial screening measure in a longitudinal cohort at risk for Alzheimer's disease. *J Alzheimers Dis Rep*. 2017;1:9-13.
20. Koscik RL, La Rue A, Jonaitis EM, et al. Emergence of mild cognitive impairment in late middle-aged adults in the Wisconsin registry for Alzheimer's prevention. *Dement Geriatr Cogn Disord*. 2014;38:16-30.
21. Han Y, Zheleznyakova GY, Marincevic-Zuniga Y, et al. Comparison of EM-seq and PBAT methylome library methods for low-input DNA. *Epigenetics*. 2022;17:1195-1204.
22. Merkel A, Fernandez-Callejo M, Casals E, et al. gemBS: high throughput processing for DNA methylation data from bisulfite sequencing. *Bioinformatics*. 2019;35:737-742.
23. Martin M. Cutadapt removes adapter sequences from high-throughput sequencing reads. *EMBnetjournal*. 2011;17(1).
24. Fong J, Gardner JR, Andrews JM, et al. Determining subpopulation methylation profiles from bisulfite sequencing data of heterogeneous samples using DXM. *Nucleic Acids Res*. 2021;49:e93.
25. Wu H, Wang C, Wu Z. A new shrinkage estimator for dispersion improves differential expression detection in RNA-seq data. *Biostatistics*. 2013;14:232-243.
26. Strimmer K. fdrtool: a versatile R package for estimating local and tail area-based false discovery rates. *Bioinformatics*. 2008;24:1461-1462.
27. Howe KL, Achuthan P, Allen J, et al. Ensembl 2021. *Nucleic Acids Res*. 2021;49:D884-D891.
28. Wilson DJ. The harmonic mean *p*-value for combining dependent tests. *Proc Natl Acad Sci U S A*. 2019;116:1195-1200.
29. Yu G, Wang LG, Han Y, He QY. clusterProfiler: an R package for comparing biological themes among gene clusters. *OMICS*. 2012;16:284-287.
30. Boyle EI, Weng S, Gollub J, et al. GO::TermFinder–open source software for accessing gene ontology information and finding significantly enriched gene ontology terms associated with a list of genes. *Bioinformatics*. 2004;20:3710-3715.
31. Javierre BM, Burren OS, Wilder SP, et al. Lineage-specific genome architecture links enhancers and non-coding disease variants to target gene promoters. *Cell*. 2016;167:1369-1384. e19.
32. Hinrichs AS, Karolchik D, Baertsch R, et al. The UCSC genome browser database: update 2006. *Nucleic Acids Res*. 2006;34:D590-D598.
33. Shigemizu D, Mori T, Akiyama S, et al. Identification of potential blood biomarkers for early diagnosis of Alzheimer's disease through RNA sequencing analysis. *Alzheimers Res Ther*. 2020;12:87.
34. Ginestet C. ggplot2: elegant graphics for data analysis. *J Roy Stat Soc A*. 2011;174:245.
35. Xiao N, ggsci: Scientific journal and Sci-Fi themed color palettes for 'ggplot2'_. R package version 2.9 ed2018.
36. Wilke C, cowplot: Streamlined plot theme and plot annotations for 'ggplot2'_. R package version 1.1.1 ed2020.
37. Hicks SC, Irizarry RA. methylCC: technology-independent estimation of cell type composition using differentially methylated regions. *Genome Biol*. 2019;20:261.
38. Bellenguez C, Kucukali F, Jansen IE, et al. New insights into the genetic etiology of Alzheimer's disease and related dementias. *Nat Genet*. 2022;54:412-436.
39. Kulminski AM, Jain-Washburn E, Loiko E, et al. Associations of the APOE epsilon2 and epsilon4 alleles and polygenic profiles comprising APOE-TOMM40-APOC1 variants with Alzheimer's disease biomarkers. *Aging (Albany NY)*. 2022;14:9782-9804.
40. Hoogmartens J, Cacace R, Van Broeckhoven C. Insight into the genetic etiology of Alzheimer's disease: a comprehensive review of the role of rare variants. *Alzheimers Dement (Amst)*. 2021;13:e12155.
41. Strickland SL, Reddy JS, Allen M, et al. MAPT haplotype-stratified GWAS reveals differential association for AD risk variants. *Alzheimers Dement*. 2020;16:983-1002.
42. Emrani S, Arain HA, DeMarshall C, Nuriel T. APOE4 is associated with cognitive and pathological heterogeneity in patients with Alzheimer's disease: a systematic review. *Alzheimers Res Ther*. 2020;12:141.
43. Amaral P, Carbonell-Sala S, De La Vega FM, et al. The status of the human gene catalogue. ArXiv. Preprint posted online March 24, 2023. https://pubmed.ncbi.nlm.nih.gov/36994150/
44. Blue EE, Thornton TA, Kooperberg C, et al. Non-coding variants in MYH11, FZD3, and SORCS3 are associated with dementia in women. *Alzheimer Dement*. 2021;17:215-225.
45. Kamboh MI. Genomics and functional genomics of Alzheimer's disease. *Neurotherapeutics*. 2022;19:152-172.
46. Fuhrer TE, Palpagama TH, Waldvogel HJ, et al. Impaired expression of GABA transporters in the human Alzheimer's disease hippocampus, subiculum, entorhinal cortex and superior temporal gyrus. *Neuroscience*. 2017;351:108-118.
47. Ando K, De Decker R, Vergara C, et al. Picalm reduction exacerbates tau pathology in a murine tauopathy model. *Acta Neuropathol*. 2020;139:773-789.
48. Kim S, Park HJ, Cui X, Zhi D. Collective effects of long-range DNA methylations predict gene expressions and estimate phenotypes in cancer. *Scientific reports*. 2020;10:3920.
49. Tang X, Tena J, Di Lucente J, et al. Transcriptomic and glycomic analyses highlight pathway-specific glycosylation alterations unique to Alzheimer's disease. *Scientific reports*. 2023;13:7816.
50. Kane AE, Sinclair DA. Epigenetic changes during aging and their reprogramming potential. *Crit Rev Biochem Mol Biol*. 2019;54:61-83.
51. Kerschbamer E, Arnoldi M, Tripathi T, et al. CHD8 suppression impacts on histone H3 lysine 36 trimethylation and alters RNA alternative splicing. *Nucleic Acids Res*. 2022;50:12809-12828.
52. Kohli RM, Zhang Y. TET enzymes, TDG and the dynamics of DNA demethylation. *Nature*. 2013;502:472-479.

53. Cho JW, Shim HS, Lee CY, et al. The importance of enhancer methylation for epigenetic regulation of tumorigenesis in squamous lung cancer. *Exp Mol Med*. 2022;54:12-22.
54. Lin X, Li L, Liu X, et al. Genome-wide analysis of aberrant methylation of enhancer DNA in human osteoarthritis. *BMC Med Genomics*. 2020;13:1.
55. Pai S, Li P, Killinger B, et al. Differential methylation of enhancer at IGF2 is associated with abnormal dopamine synthesis in major psychosis. *Nature communications*. 2019;10:2046.
56. Hu Y, Huang K, An Q, et al. Simultaneous profiling of transcriptome and DNA methylome from a single cell. *Genome biology*. 2016;17:88.
57. Bennett DA, Buchman AS, Boyle PA, Barnes LL, Wilson RS, Schneider JA. Religious orders study and rush memory and aging project. *Journal of Alzheimer's disease : JAD*. 2018;64:S161-S189.
58. Iturria-Medina Y, Adewale Q, Khan AF, et al. Unified epigenomic, transcriptomic, proteomic, and metabolomic taxonomy of Alzheimer's disease progression and heterogeneity. *Sci Adv*. 2022;8:eabo6764.
59. Sims D, Sudbery I, Ilott NE, Heger A, Ponting CP. Sequencing depth and coverage: key considerations in genomic analyses. *Nat Rev Genet*. 2014;15:121-132.
60. Mietelska-Porowska A, Wojda U. T lymphocytes and inflammatory mediators in the interplay between brain and blood in Alzheimer's disease: potential pools of new biomarkers. *J Immunol Res*. 2017;2017:4626540.
61. Gate D, Saligrama N, Leventhal O, et al. Clonally expanded CD8 T cells patrol the cerebrospinal fluid in Alzheimer's disease. *Nature*. 2020;577:399-404.
62. DeMaio A, Mehrotra S, Sambamurti K, Husain S. The role of the adaptive immune system and T cell dysfunction in neurodegenerative diseases. *J Neuroinflammation*. 2022;19:251.

SUPPORTING INFORMATION

Additional supporting information can be found online in the Supporting Information section at the end of this article.

How to cite this article: Breen C, Papale LA, Clark LR, et al. Whole genome methylation sequencing in blood identifies extensive differential DNA methylation in late-onset dementia due to Alzheimer's disease. *Alzheimer's Dement*. 2024;20:1050–1062. https://doi.org/10.1002/alz.13514